EFFECT OF DYNAMIC STRAIN AGING ON HIGH TEMPERATURE LOW CYCLE FATIGUE OF FERRITIC DUCTILE CAST IRON

Hayato Mouri*[1], Morihito Hayashi *[2], Wilfried Wunderlich *[3]

*1 Graduate student, Unified Graduate School of Engineering, Tokai University,
*2 Professor, Dr. Eng., Department of Mechanical Engineering, Faculty of Engineering, Tokai University,
*3 Associate Professor, Dr. Eng., Department of Material Science, Faculty of Engineering, Tokai University,
1117 Kitakaname Hiratsuka, Kanagawa Japan.
(hayato_mori@hotmail.com)

ABSTRACT

Ferrite ductile cast iron (FCD400) is widely used as an industrial material with an excellent properties mechanical property because of its low cost. The advanced mechanical properties of ductile cast iron including fatigue at the high temperature have been investigated and clarified.(1) ~ (6) In low cycle fatigue, the fatigue life can be predicted by Coffin-Manson's model, when the S-N curve is measured, and the ductile index as a material constant of 0.5 and the ductile coefficient are related directly to the so-called plastic deformation capacity of material. In this case, the low cycle fatigue life time is dominated by the elongation rate, which is 20% at 293K, but reduces to about 9% at 473K, the temperature, which is within the range of dynamic strain ageing (DSA), the phenomenon of fluctuating stress due to mobile solid solution atoms. In this study LCF-experiments at 293K, 413K, and 473K were compared. As a result, the fatigue life can be predicted using the Manson-Coffin rule when the elongation rate by the plastic strain is included. Under the influence of DSA three different parameter sets for different temperature ranges are necessary, so that non-linear deviations are almost negligibly.

KEY WORDS

Ductile cast iron, high temperature low - cycle - fatigue, plastic strain, elastic strain, total strain range, dynamic strain ageing

INTRODUCTION

The ferritic ductile iron (FCD400) is widely used as industrial material, because it has superior mechanical properties and low price. It is also used as heat resistant material for machinery parts applied at elevated temperature. Therefore, recently, advanced mechanical properties of ductile cast iron including fatigue at the high temperature have been investigated and clarified (1) ~ (6).
In low cycle fatigue, the S-N curve is presented by the relation of plastic strain to the number of cycles as fatigue life, which can be predicted by Coffin-Manson's model. In this model, the ductile index is appointed as a material constant of 0.5 and the ductile coefficient is related directly to the so-called plastic deformation capacity of material. Namely, the low cycle fatigue life shall be dominated by the elongation rate. Concerned with it, one of authors reported that[1)] the elongation is 20% at room temperature, but reduces to about 9% at 473K, a temperature within the range of dynamic strain ageing (DSA), which is the phenomenon of fluctuating stress due to mobile solid solution atoms.. Moreover, according to the latest study [2)], the elongation is 15% at 473K compared to 20% at 293K.
So, in the study, strain controlled high temperature low-cycle fatigue tests were carried out on ferritic

cast iron at 473K in air and the result was compared with that at 293K, aiming to clarify the effect of elongation and DSA on the fatigue life. Particularly, this paper considers the influence of the DSA effect on cyclic stress and cyclic plastic strain which causes deviations of the Manson–Coffin's model in the plastic strain range versus number of cycles between 293K, 413K and 473K.

EXPERIMENT AND MATERIAL

Test material

Round test pieces (diameter 30mm, length 210mm) of FCD400 (Japan Industrial Standard) were used for the test. The chemical composition of specimen and microstructure of the transverse section is shown in table 1 and figure 1. The tension test and fatigue test specimens were processed as shown in Figure 2.

C	Si	Mn	P	S	Cr	Mg	Zn	Al	Sn	Cu
3.83	2.55	0.18	0.023	0.008	0.029	0.038	0	0.003	0	0.04

Table.1 Chemical composition of specimen

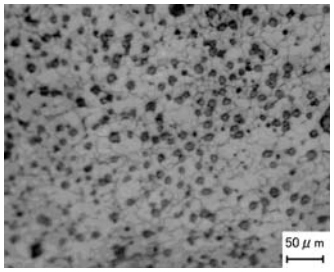

Fig.1 Microstructure of transverse section

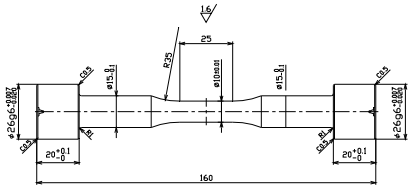

Fig.2 Geometry of fatigue specimen

Figure.3 shows the Stress – Strain diagram as obtained from the tension test at 413K and 473K, as black and hatched lines, respectively. The data are also shown in table.2. So, it was confirmed that the test pieces lie within the range of the Japan Industrial Standard (JIS).

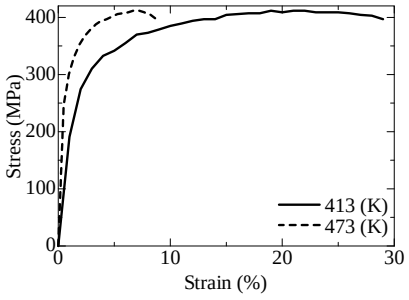

Fig.3. Stress – Strain diagram

	Specimen			FCD400 (JIS)
Temperature (K)	293	413	473	
Tensile Strength (MPa)	476	410.6	411	400～500
0.2% proof strength (MPa)	381	314	314	Over 250
Elongation (%)	28	17	8	≧18
Rate of reduction (%)	13	21	18	
Young's ratio (GPa)	235	103	101	

Table.2 Tensile properties on FCD400

Test condition

In this study, the high temperature low cycle fatigue tests were carried out by a computerized hydraulic servo pulsar EHF-ED100kN-TF-20L fabricated by Shimazu. The test was under taken at 473K, at a total strain range selected from 0.5% to 2%, and at a constant strain rate of 0.4 %/s with triangular shaped cycles applied to specimens with gage length of 15mm and diameter of 10mm. During test load, strain, number of repeated cycle and temperature of gage length were detected and recorded.

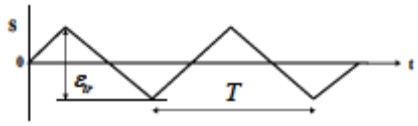

Fig.4 pulsating sawtoothed strain wave for strain controlled fatigue test.

Specimen	FCD400
Test environment	R.T. in Air & 473K in Air
Wave form of strain	Sawtooth
Total strain range, $\varepsilon_{tr(\%)}$	0.5 – 2
The rate of strain $\dot{\varepsilon}$ (%/s)	0.4
Strain mesurement	Displacement meter (GL=15mm)

Table .3 Test Condition

$$\dot{\varepsilon} = 2\varepsilon_{tr}/T = 2\varepsilon_{tr} f \ \ldots (1)$$

T in the expression is the cycle period of the strain, and *f* is the frequency.

EXPERIMENT RESULT AND DISCUSSION

The plastic strain is obtained from the hysteresis loop to expression (2).

$$\varepsilon_{tr} = \varepsilon_{el} + \varepsilon_{pl} \quad (2)$$

Strain controlled fatigue test results of FCD400 are shown in table.4. Normally, the fatigue life is calculated using the equation (3)

$$\varepsilon_{pl} = C_p \cdot N_f^{\kappa_p} \quad (3)$$

with the parameters $C_p = 104, \kappa_P = 0.82$ at 293K (4).

These parameter set is valid for the temperature range, where no DSA effect occurs (293K). At 473 K the steeper slope in Fig. 6 suggests these parameters are not valid any more: The fatigue life according to expression (3) at a total strain of 2% would be 179 cycles, but in the experiment it is 610 cycles. Because neither the index nor the coefficient includes the correct temperature dependence as in the experiment, a different set of parameters for the Manson-Coffin rule is necessary for the temperature range, where DSA occurs. All data can be fitted with negligible non-linear deviations at very high stresses with different sets of parameter as calculated according to expression (3) as

$$C_p = 201, \kappa_P = 0.83 \quad \text{at 413K,} \quad C_p = 421, \kappa_P = 0.89 \quad \text{at 473K. (5)}$$

The experimental result shown in Fig.5 is the diagram for “Plastic strain versus Fatigue life”. The data at 473K and 413K are within the scattering conform to each other and have significantly longer fatigue life times than at 293K. Also the plastic strain of 473K and 413K are larger than plastic strain at 293K. These experimental data are different from normal behavior, where the fatigue life is short when the plastic strain is large. From Fig.5 it is also deduced, that the fatigue life becomes almost the same in the case of low plastic strain independent of the temperature. It is considered that this behavior can be explained by less effective hardening: Dislocations are not yet pulled far enough to be fixed by carbon atoms, so that the Cottrell cloud is not yet formed. Or in other words DSA is not occurring for small plastic strain.

For the confirmation of the presence of DSA, tensile tests at 473K and 413K were also performed. The result is, that at the same strain rate $\dot{\varepsilon}$= 0.4%s^{-1} as in the fatigue experiments the DSA phenomenon occurs. However, when the tensile test was performed by interrupting a fatigue test of total strain of 2% after ten cycles at 473K, DSA could not be confirmed. In this tensile test, the elongation rate until fracture was measured as 40%, much larger than at the tensile test at virgin specimens (9%). Moreover, the yield stress is 450MPa at tensile test after 10 fatigue cycles but the yield stress at virgin specimens is almost 410MPa. It is considered that the carbon atoms in solid solution are trapped in cores of immobile dislocations formed during the first fatigue cycles. Through this, mobile dislocations are not hindered anymore by carbon atoms and this explains the longer life time at high stress levels (Fig. 6) compared to 293K.

Fig.6 shows the corresponding diagram of stress versus fatigue life with the following values: The

fatigue life is 186352 cycles at a stress value of 268 MPa at 293K, while at the same stress at 413K the fatigue life is 102829 cycles and at 473 K 38560 cycles, or in other words, the life time is about 1/4 shorter at 413K compared to 293K, but at 473K only half. Moreover, when the fatigue life at 398MPa is compared, (959 cycles at 293 K, 392 cycles at 413K) it decreased about 1/3. All data points are lying on a straight line, therefore the Manson-Coffin parameter can be estimated as shown above in (5). However, the data at 413 K are shifted towards shorter cycles. At 473 K the data are almost the same as at 293 K, but the slope is slightly steeper with a cross over at 336MPa. The hysteresis loops in Fig.7 were generated from the fatigue test data. At a total strain 2% (Fig.7a) the maximum and minimum stresses at 293K are almost constant, confirming a saturation, while at 473 K there is an inclined slope. The magnified curve in Fig. 7c confirmed that there is no DSA phenomena at all three temperatures. However, at low total strain values (Fig. 7 b, d) the DSA behavior can be observed at 413 K as well as at 473 K.

As a summary, the characteristic occurrence of fatigue behavior seen in the experimental data can be explained by the dynamic strain aging. A complete solid solution hardening works at 293K up to 400 K according to literature data [1], because the dislocation velocities are faster than the diffusion of the carbon atoms. At 400 K up to 473K, because the dynamic strain aging exists at low stress levels, the solid solution of the carbon atom rearrange immediately according to the dislocation movement, in other words DSA happens because of the competition of almost the same velocities of both, the dislocations and the diffusion of the carbon atoms. This was deduced from tension test on cast iron in the range of 423 K~573 K [2] ~ [3]. At high stress levels, DSA does not occur, because the numbers of dislocations or the dislocation velocities are so high, that the trapped carbon atoms cannot contribute to any hardening effect. At higher temperatures (> 573K) the solid solution hardening mechanism works perfect, because than the carbon diffusion is faster than the dislocations.

The Manson-Coffin rule is based on continuum mechanics and according to the data in the three temperature ranges (293-400K, 400-573K, >573K) different micro-structural features occur. So, it is inevitably, that we need three different parameter sets for the materials modeling, which is however sufficient to forecast reliable fatigue properties. Further research needs to clarify the strain rate dependence.

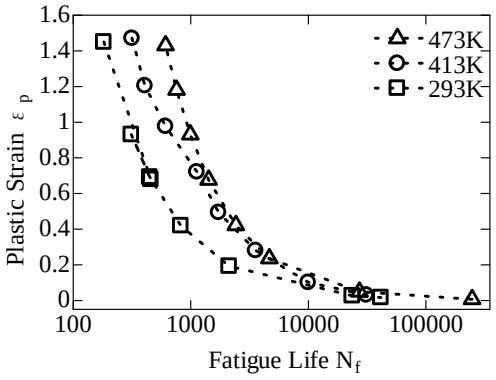

Fig.5 Diagram Plastic strain vs. Fatigue life

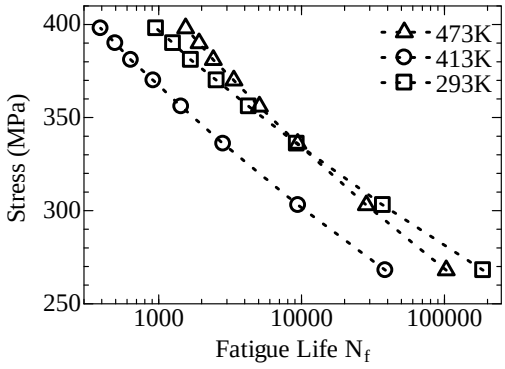

Fig.6 Diagram Stress vs. Fatigue life

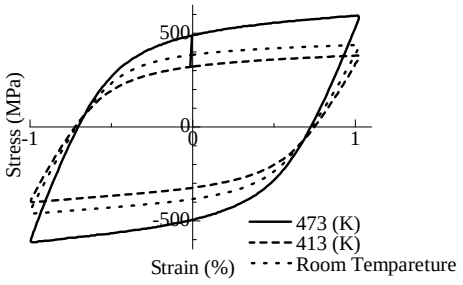

(a) 2% of strain

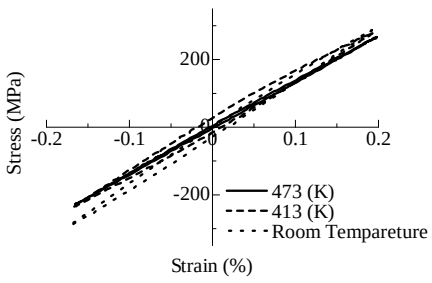

(b) 0.5% of strain

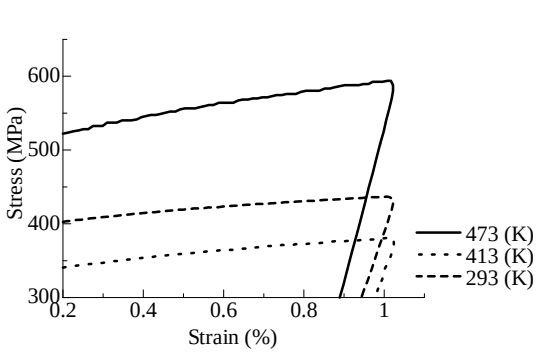

(c) 2% of strain DSA part

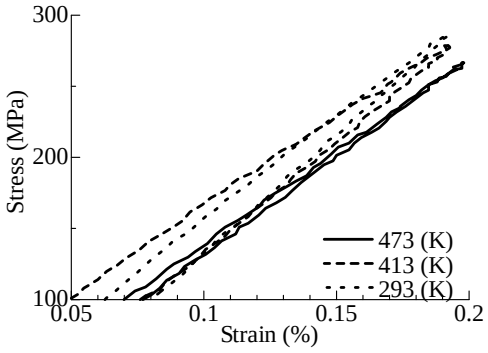

(d) 0.5% of strain DSA part

Fig.7 Hysterisis loop

Speci.No.	f (Hz)	$\Delta\varepsilon_t$ (%)	$\Delta\varepsilon_t$ Actual (%)	$\Delta\varepsilon_p$ (%)	$\Delta\varepsilon_e$ (%)	σ_{max} (MPa)	σ_{min} (MPa)	σ_r (MPa)	σ_a (MPa)	N_f (Cycle)
473 (K)										
1	0.40	0.5	0.36	0.0070	0.5070	193	−238	431	216	247048
2	0.33	0.6	0.48	0.0492	0.5508	307	−342	649	324	27221
3	0.25	0.8	0.72	0.2357	0.5643	399	−424	823	412	4659
4	0.20	1	0.97	0.4221	0.5779	433	−455	888	444	2415
5	0.16	1.25	1.23	0.6768	0.5732	460	−480	940	470	1419
6	0.13	1.5	1.49	0.9315	0.5685	479	−497	976	488	990
7	0.11	1.75	1.74	1.1812	0.5688	493	−510	1002	501	757
8	0.10	2	2.00	1.4309	0.5691	504	−520	1024	512	610
413 (K)										
9	0.40	0.50	0.36	0.0314	0.4686	225	−332	534	267	38560
10	0.33	0.60	0.51	0.1020	0.4980	275	−312	612	306	9450
11	0.25	0.80	0.75	0.2809	0.5191	318	−350	679	339	2824
12	0.20	1.00	0.98	0.4947	0.5053	343	−366	716	358	1438
13	0.16	1.25	1.25	0.7217	0.5283	359	−383	741	370	917
14	0.13	1.50	1.51	0.9773	0.5227	372	−392	761	380	639
15	0.11	1.75	1.76	1.2054	0.5446	381	−400	775	387	497
16	0.10	2.00	2.02	1.4716	0.5284	389	−407	788	394	392
Room Temperature										
17	0.40	0.50	0.36	0.0168	0.4832	302	−294	596	298	41396
18	0.33	0.60	0.46	0.0266	0.5734	316	−310	627	313	23649
19	0.25	0.80	0.72	0.1929	0.6071	380	−379	759	379	2119
20	0.20	1.00	0.97	0.4201	0.5799	404	−406	811	405	822
21	0.16	1.25	1.25	0.6921	0.5579	420	−424	844	422	447
22	0.13	1.50	1.51	0.9313	0.5687	430	−434	864	432	312
23	0.11	1.75	1.77	0.6795	0.5705	420	−423	843	421	458
24	0.10	2.00	2.02	1.4502	0.5498	444	−450	893	447	182

Table.4 Strain controlled fatigue test results of FCD400 (waveform: sawtooth)

FRACTOGRAPHY

The fractography by SEM was also performed as seen in typical fractographs Fig.8 (a, b, c) under the total strain 2% condition. The photographs, taken after LCF experiments at three different temperatures, show the points of crack initiation, which occurs at several locations on the surface at about 80% of the life time. The fracture surfaces in all specimens are flat, perpendicular to the stress direction, indicating a mainly brittle manner of fracture. From the fractographies it is deduced, that the interface to graphite particles is the initiation point of the crack because dimple pattern occur always around the particles. Dimple pattern, river pattern and striation have the same morphology at all temperature and also the coexistence of river pattern and striations could be confirmed in all cases (Fig. 8 a-c). The area which is covered by striations is larger for the specimens deformed at 0.5% of total strain, while for those deformed at 2% it is smaller.
The conclusion from these observations is that the crack initiation and propagation in the late stage of fatigue life occurs under all conditions in the same manner. Hence, for the modeling of the Manson-Coffin law it has no influence.

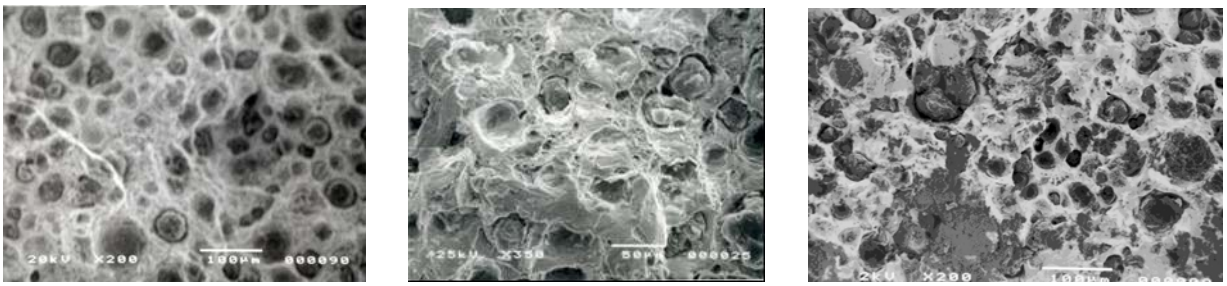

(a) 293K (b) 413K (c) 473K

Fig.8 SEM micrographs of LCF fatigue cracks (2% of total strain)

CONCLUTION

In this research, low cycle fatigue tests were performed on ferrite ductile cast iron at room and elevated temperatures (293 K, 413 K and 473 K) under ambient atmosphere. The obtained results are as following.

1. The fatigue life time increased at 413 K and 473 K compared to 293 K at high plastic strain rates.
2. In the tensile tests at 413 K and 473 K the DSA phenomena occurs regardless of the height of the strain, but at fatigue test DSA occurs only at cycles with large strain.
3. At 413 K the fatigue life time decreased compared to 293 K for all stress levels, and at 473 K it decreases only at low stress levels.
4. The fatigue life can be predicted by the Manson-Coffin rule with the parameters Cp=0.09, n=0.65 at 293 K, and for other temperatures with different sets of fit parameter.
5. Fatigue behavior of ductile cast iron can be distinguished in three different temperature ranges (293 – 400 K, 400 – 573 K, > 573 K) according to the competition of dislocation speed and diffusion speed of carbon atoms. In the middle range, where both velocities are compatible, dynamic strain aging (DSA) occurs. The influence of embrittlement due to large dislocation velocities could also be confirmed.

REFERENCE

1) K. Chijiiwa, M. Hayashi, Mechanical properties of ductile cast iron at temperature in the region of room temperature to liquid, Imono Vol.51 No.7, (2004), pp. 395 – 400.
2) O. Yanagisawa, M. Maruyama, K. Arii, T. Ishigai, M.Konishi, Tensile and Fatigue Strength and Fracture of Spheroidal Graphite Cast Iron with Ferrite Matrix in the Temperature Range between Room Temperature and 500°C, Imono Vol.52 No.6, (1980),, pp. 331 – 336..
3) K.Yasue, H.Matsubara, M.Isotani, Y.Kondo, Temperature Dependence of Low Cycle Fatigue Life in Cast Iron, Imono Vol.52 No.12, (1980),, pp. 669 – 674.
4) M. Hayashi, Thermal Fatigue Life prediction-Verification of Coffin-Manson's law in the phase transformation range of ferrite matrix ductile cast iron, Material-Prüfung, Vol.46, No.7-8, (2005), pp374-pp.378.
5) M. Hayashi and H. Mouri, Monosemousness of Thermal Plastic Strain on Thermal Fatigue Life in Ferrite Ductile Cast Iron, Journal of Solid Mechanics and Materials Engineering, Vol. 1 (2007) , No. 5 pp.711-718.
6) S. Harada, Y.Akiniwa, T.Ueda, M. Yano, The effect of nodule count on the low – cycle fatigue life of ferritic ductile cast iron, Trans. of The Japan Society of Mechanical Engineers Vol.62 No.572A, (1994), pp.952 – 959.